Dalton Transactions

Accepted Manuscript

This is an *Accepted Manuscript*, which has been through the Royal Society of Chemistry peer review process and has been accepted for publication.

Accepted Manuscripts are published online shortly after acceptance, before technical editing, formatting and proof reading. Using this free service, authors can make their results available to the community, in citable form, before we publish the edited article. We will replace this *Accepted Manuscript* with the edited and formatted *Advance Article* as soon as it is available.

You can find more information about *Accepted Manuscripts* in the Information for Authors.

Please note that technical editing may introduce minor changes to the text and/or graphics, which may alter content. The journal's standard Terms & Conditions and the Ethical guidelines still apply. In no event shall the Royal Society of Chemistry be held responsible for any errors or omissions in this *Accepted Manuscript* or any consequences arising from the use of any information it contains.

ROYAL SOCIETY OF CHEMISTRY

www.rsc.org/dalton

Please do not adjust margins

Journal Name

ARTICLE

Fabrication and characterization of highly sensitive hydroquinone chemical sensor based on iron-doped ZnO nanorods

Received 00th January 20xx,
Accepted 00th January 20xx

DOI: 10.1039/x0xx00000x

www.rsc.org/

Ahmad Umar,[a,b,*] Ali Al-Hajry,[a,c] Rafiq Ahmad,[d] S.G. Ansari[e], Mohammed Sultan Al-Assiri[a,c], Hamed Algarni[f]

Herein, we report the development of a simple and highly sensitive hydroquinone (HQ) chemical sensor based on an electrochemically activated iron-doped (Fe-doped) zinc oxide nanorods (ZnO NRs) modified screen-printed electrode (SPE). The Fe-doped ZnO NRs were prepared by hydrothermal process and their morphological, crystal, compositional and optical properties were characterized in detail. The detailed characterizations showed that the NRs are densely grown, well-crystalline and possess wurtzite hexagonal phase. The fabricated HQ electrochemical sensor exhibited high sensitivity of 18.60 µA mM-1 cm-2 and a very low experimental detection limit of 0.51 µM. Our results demonstrate that simply prepared doped ZnO nanomaterials are promising candidates to fabricate high-sensitive electrochemical sensors.

Introduction

Researchers have used extensively screen-printed electrodes (SPEs) as an effective electrode system for the fabrication of disposable miniaturized electrochemical sensors to detect various chemicals and biomolecules. In order to tailor or improve the performance, SPEs have been modified using various nanomaterials, ions, polymers and others.[1-3] It is evident from literatures that recent development in dimensionality, functionality of nanostructured materials has opened opportunities and possibilities for tuning application-suited properties and material characteristics.[4] For example, extensive research has been done to tailor the band gap and optical properties of metal oxides by doping with various metals. A step further, bimetal have also been used for synthesizing novel material including perovskite materials. This effort has led to develop material suited for particular application including biosensors, dye sensitized solar cells, pesticide sensors and other toxic element sensors. SPEs have made easier to develop electrochemical sensor just by printing/depositing film over the working electrode and the whole trip can be used as the sensing element offering ease of fabrication and low cost device.

Therefore, investigations of novel materials for device fabrication/development are very important for technological advancement.[5-10] Metal oxides are known to offer flexibility for doping by simple and economic synthesis route to tailor the material properties. With the help of solution technique, it became easy to convert precursors of single or bi-metallic oxides with homogenous size, shape, distribution and phase purity simply by controlling the aggregation.

Increasing automation with industrial growth end up with introducing chemical contaminants into the environment besides producing the value added products. Many of these contaminants are toxic having long term adverse impact. These being source of great concern, requires continuous detection, monitoring, detoxification and environmental remediation. HQ is one such contaminant widely used in pharmaceutical and industrial products.[11] Since it is soluble in water, it requires to be detected with sufficient sensitivity using suitable sensing electrodes to protect against the threat to human health. Due to its unregulated use as 'skin lightener' in cosmetics and long term effect on human health, there is a debate and controversy on its total ban in many European countries, USA, China etc. However, until today it has not been classified as carcinogen. Its continuous use or exposure results in de-pigmentation of skin, which itself can lead to increased possibility of cancer. Therefore, an improvement is needed to develop a convenient, simple and rapid analytical method/device for the detection of lowest possible levels of HQ.[11,12]

The conventional techniques used for detection and measurements are chemiluminescence, high performance liquid chromatography (HPLC), spectrophotometry and others. The electrochemical methods for HQ sensing are fairly new and needs to be developed, having numerous advantages such

[a] Promising Centre for Sensors and Electronic Devices, Najran University, P.O. Box 1988, Najran, 11001, Kingdom of Saudi Arabia.
E-mail: ahmadumar786@gmail.com, Phone No.: +966-534574597
[b] Department of Chemistry, Faculty of Sciences and Arts, Najran University, Najran University, P.O. Box 1988, Najran, 11001, Kingdom of Saudi Arabia.
[c] Department of Physics, Faculty of Sciences and Arts, Najran University, Najran University, P.O. Box 1988, Najran, 11001, Kingdom of Saudi Arabia.
[d] School of Semiconductor and Chemical Engineering, Nanomaterials Processing Research, Chonbuk National University, 567 Baekje-daero, Deokjin-gu, Jeonju 561-756, Republic of Korea.
[e] Centre for Interdisciplinary Research in Basic Sciences, Jamia Millia Islamia, New Delhi-110025, India.
[f] Department of Physics, Faculty of Science, King Khalid University, P. O. Box 9004, Abha, Kingdom of Saudi Arabia

Dalton Transactions Accepted Manuscript

Please do not adjust margins

as simplicity, efficiency, reduced costs, selectivity and most importantly ease of analysis without elaborated sample preparation and pre-procedures.

A number of nano-materials were efficiently deployed as electron mediators/matrix for the development of different reliable electrochemical sensors.[11-15] Among these, ZnO, conducting polymers, graphene and carbon has been reported for electrochemical detection of HQ. For example, Silva and co-authors modified carbon paste electrode with 3-n-propyl-4-picolinium chloride silsesquioxane polymer for detection of HQ isomers.[16] In an another report, Han and co-worked employed electrochemically reduced hybrid material, ER (GO-TT-CNT) that was prepared by in-situ polymerization of graphene oxide (GO), multi-walled carbon nanotube (CNT), and terthiophene (TT) for detection of HQ in a range of pH 4.04 - 9.01.[17]

Very recently, attempts have been made to utilize ZnO nanomaterials for variety of applications, as they are favourable material due to ease of fabrication, high chemical stability, high surface area and high electron transfer capability.[18-20] Also, various types of dopant could be used to enhance the performance of ZnO NRs, which may offer an effective method to enhance the optical, electrical and electrochemical properties of ZnO NRs for practical applications.[21] In one of our earlier report, Ce-doped ZnO NRs were used as effective electron mediator for HQ detection.[22] In another report, Zhang and co-authors used modified core-shell magnetic nanoparticles supported on carbon paste for such sensor the laccase was covalently immobilized on the magnetic nanoparticles by glutaraldehyde.[23] In a recent research article published by Li and co-workers, fabricated novel biosensor on a composite of ZnO loaded carbon nanofibers, laccase and Nafion that resulted in electrocatalysis of HQ.[24] Previously, Fe-doped ZnO NRs have been extensively used not only for sensing applications but also as high performance UV photodetectors and for ferromagnetism, catalysis, etc.[25] In addition to these similarity in ionic radii and Pauling electro-negativities with Zn, substitution of Fe-ion can be to the higher concentrations resulting in increased ionic/electronic conduction as compared to that of undoped ZnO[25f]. However, to the best of our knowledge, there is no report on utilization of Fe-doping in ZnO for the fabrication of a highly sensitive HQ sensor to a category of VOC sensor.

With the above background, a highly sensitive HQ sensor is developed using Fe-doped ZnO NRs synthesized through solution chemistry. The synthesized material was used as a working electrode on SPE and the electrochemical sensing characteristics were determined using a potentiostat from 0.78mM to 5mM of HQ at room temperature.

Experimental

Materials. Zinc chloride dihydrate ($ZnCl_2.2H_2O$), hexamethylenetetramine (HMTA), Iron chloride ($FeCl_2$), ammonium hydroxide (NH_4OH) and hydroquinone were purchased from Sigma-Aldrich and used without further purification or distillation. For synthesis and sensing experiments, de-ionized (DI) water (resistivity of 18MΩ, Millipore) was used as solvent and solution preparation.

Synthesis of Fe-doped ZnO NRs. The Fe-doped ZnO NRs were synthesized by a simple hydrothermal process. In a typical experiment, first, 0.1M $ZnCl_2.2H_2O$ and 0.01M $FeCl_2$ were dissolved in DI water and then mixed at room-temperature via stirrring for 25 min. After 25 min of contineous stirring, aqueous solution of 0.1M HMTA, made in 25 ml DI water, was added in the previous solution and the resultant solution was again stirred for 30 min. The pH of the solution was adjusted to 10 by adding few drops of NH_4OH. For crystal growth of ZnO NRs using $ZnCl_2$, the ideal pH is ~10, which facilitates the creation of these ZnO nanostructures. As, OH^- ions are strongly attracted to the positively charged zinc ions and surfaces, which causes the zinc to form ZnO bonds in a long chain rather than into a plate. If pH is too low, there will not be enough OH-ions to force the zinc into intermolecular bonds, which will cause it to form plates or film. If pH is too high, intermolecular bonding can grow out of control and cause bond formation to become unselective in preferential orientation, which would cause undesired nanostructure growth and decrease in uniformity.[26] Finally, the above obtained solution was vigorously stirred for 30 min then transfered to teflon lined autoclave and heated upto 160 ºC for 6 h. After completion of reaction, the obtained product was collected and washed with DI water and ethanol, sequentially and dried at 50 ºC. The mechanism for the synthesis of the Fe-doped ZnO NRs using HMT can be summarized in the following equations:

$$(CH_2)_6N_4 + 6H_2O \rightarrow 6COH_2 + 4NH_3 \quad (1)$$

$$NH_3 + H_2O \rightarrow NH_4^+ + OH^- \quad (2)$$

$$ZnCl_2 . 2H_2O \rightarrow Zn^{2+} + 2Cl^- + 2H_2O \quad (3)$$

$$Zn^{2+} + 2OH^- \rightarrow ZnO + H_2O \quad (4)$$

$$FeCl_2\,(aq) \rightarrow Fe^{2+}\,(aq) + 2Cl^-\,(aq) \quad (5)$$

$$2Fe^{2+} + 6OH^- \rightarrow Fe_2O_3 + 3H_2O \quad (6)$$

Here, HMT plays a very complicated role in the solution during the hydrothermal process,[27] but it supplies OH^- ions to the Zn^{2+} and Fe^{2+} ions to form Zn-O and Fe-O bonds here, respectively. Thereby, Fe^{2+} ions substitute the Zn lattice sites during the growth of ZnO NRs.

Characterizations of Fe-doped ZnO NRs. The morphology of as-synthesized material were characterized by field emission scanning electron microscopy (FESEM; JEOL-JSM-7600F) attached with energy dispersive spectroscopy (EDS) and transmission electron microscopy (TEM, JEOL-JEM-2010) equipped with selected area electron diffraction (SAED). Crystallinity and crystal phases of the synthesized materials were examined by X-ray diffraction (XRD; PAN analytical Xpert Pro.), measured with Cu-Kα radiations (λ = 1.54178 Å) in the range of 10-80^o with the scan speed of 8^o/min. The optical properties were studied by obtaining UV-Vis spectrum (Perkin Elmer Lambda 950) while information about functional bonds were obtained by acquiring FTIR spectrum using Perkin Elmer's FTIR spectrometer.

Dalton Transactions Accepted Manuscript

This journal is © The Royal Society of Chemistry 20xx

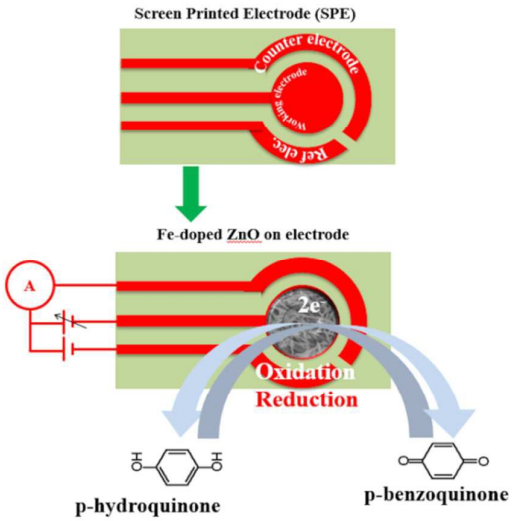

Fig. 1 Schematic representation of screen printed electrode (SPE) and HQ chemical sensing mechanism using Fe-doped ZnO NRs.

Fabrication of HQ electrochemical sensor based on Fe-doped ZnO NRs. The HQ electrochemical sensor was fabricated on screen printed electrode (SPE) containing working, counter and reference electrodes fabricated on glass epoxy PCB with gold coating. The as-synthesized Fe-doped ZnO NRs were casted on screen-printed working electrode (surface area 12.57 mm^2). Prior to the film printing, SPE was degreased and ultrasonically cleaned in distilled water. A thick paste of NRs was prepared by mixing with butyl carbitol acetate (BCA) and then casted on the screen-printed working electrode. The scheme of the electrode is shown as Fig. 1. This was allowed to settle and dried at 60±5ºC for 4-6 hrs. The different concentration of HQ solution was prepared in 0.1 M phosphate buffer solution (PBS; pH=7.4). To measure the redox reaction of the synthesized material by obtaining cyclic voltammogram (CV), the IVIUM's potentiostat/galvanostat was used. The electrochemical response of different HQ concentrations (0.78, 1, 2, 3, 4 and 5 mM) prepared in 0. 1 M PBS (pH=7.4) were measured at the scan rate of 50 mV/sec in the potential range of -1.0 to 1.0 V. The prepared HQ solutions were first purged with N_2 gas for 30 minutes and then used for sensor characterization. To understand the charge transfer kinetics, scan rates was varied (10 to 100 mV/S) to obtain the CV curves at a particular HQ concentration (1 mM) and the characteristics were related with material properties.

Results and discussion

Structural properties of as-synthesized Fe-doped ZnO NRs

The morphology of the as-synthesized material was observed under FESEM and the micrograms are shown in Fig. 2(a-d) at different magnification scales. At lower magnification (Fig. 2a) large number of rods are seen grown which are densely populated. Further magnification shows typical rods with chamfered edges (Fig. 2(b) and (c)). The widths of the rods are in the range of 150-250 nm (Fig. 2d). The elemental

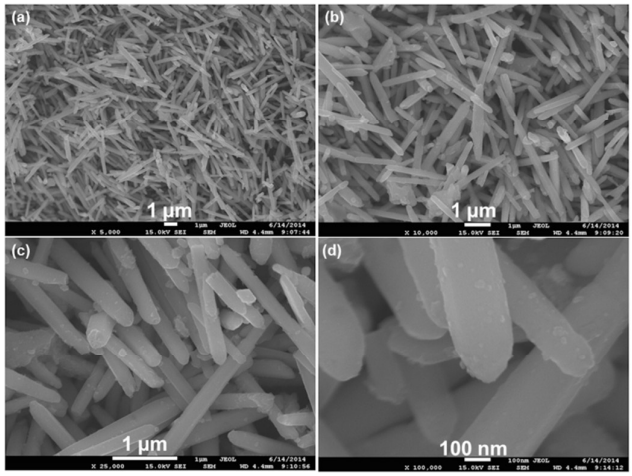

Fig. 2 Typical FESEM images of as-synthesized Fe-doped ZnO NRs.

composition of as-synthesized Fe-doped ZnO NRs was examined by EDS and result is shown in Fig. 1d. The surface of the rods seen to have some defects which can be helpful in sensing of HQ due to an increase in surface area that also leads for increased oxidation at ambient conditions.

Crystallinity and crystal phases were determined by obtaining XRD spectrum, which is shown as Fig. 3. The typical XRD pattern revealed various well-defined diffraction peaks corresponding to the lattice planes of ZnO (100), (002), (101), (102), (110), (103), (200), (112), (201), (004) and (202) planes. The diffraction pattern matched well with that of standard wurtzite hexagonal phase of ZnO (JCPDS No. 36-1451). The diffraction reflections related to other phase or materials were not found in the observed pattern which clearly revealed the complete phase formation of the doped material.

Further, the elemental analysis was carried out using EDS and the corresponding spectrum is shown as Fig. 4a & b, where peak related to zinc, oxygen and Fe were only found confirming the formation of doped compound. The optical properties were studied by obtaining the UV-Vis spectrum, shown as Fig. 4c. An absorption band is observed at 373 nm, which is close to the characteristic band value of wurtzite hexagonal pure ZnO. However, the asymmetric band shows the effect of Fe-doping. To know the information of the

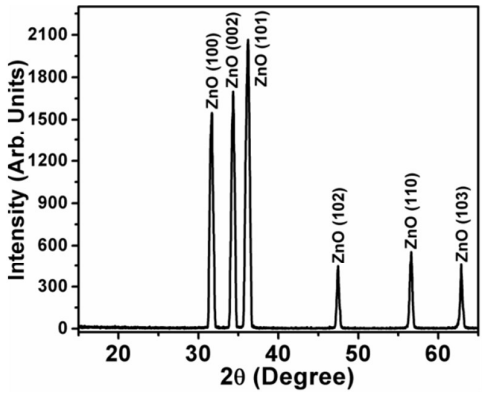

Fig. 3 Typical XRD pattern of as-synthesized Fe-doped ZnO NRs.

Dalton Transactions Accepted Manuscript

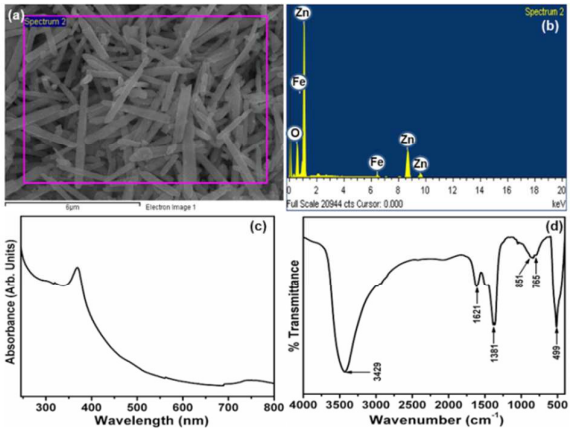

Fig. 4 Typical (a) microscopic image; (b) EDS spectrum, (c) UV-Vis. Spectrum and (d) FTIR spectrum of as-synthesized Fe-doped ZnO NRs.

chemical composition and functional bonds, FTIR spectroscopy was used and spectrum was acquired in the range of 450-4000 cm^{-1} at room-temperature (Fig. 4 (b)). The band observed at 499 cm^{-1} is correlated with metal-oxygen (M-O; Zn-O) band being in the finger print region of M-O framework. Two very small and weak bands appearing at 765 and 851 cm^{-} are due to the C-Cl stretching as chlorides were used during synthesis. The bands observed at 1381 and 1621 cm^{-1} are due to O-H and C=O vibrations. The broad band around 3249 cm^{-1} is mainly due to the O-H as the synthesis was carried out using water.[28]

All analytical data leads to the conclusion that the NRs prepared by our method possess excellent crystal quality. To confirm the crystallinity and formation of Fe-doped ZnO NRs, we characterized the un-doped and Fe-doped ZnO NRs by HRTEM measurements (Fig. 5). HRTEM images of un-doped ZnO NRs (a) showed no visible texture on its surfaces; however, Fe-doped ZnO NRs showed presence of Fe grains (c). Further, SAED pattern also confirms the formation of Fe-doped ZnO NRs. Clear diffraction rings of Fe are shown in Fig. 5d (Fe-doped ZnO NRs). It confirms that the prepared doped samples undergo a significant morphological changes induced by the Fe dopant into ZnO structure.

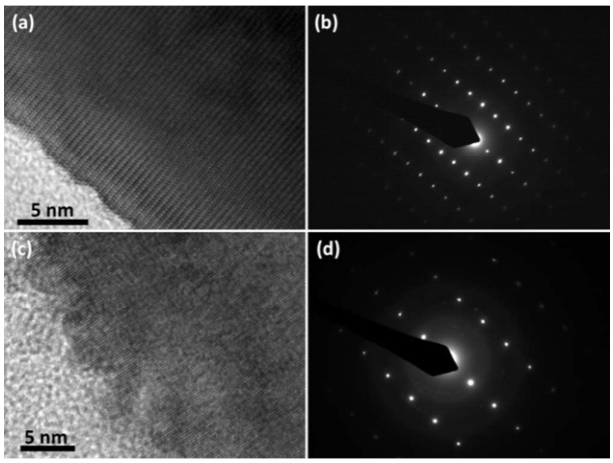

Fig. 5 HRTEM micrographs of pure ZnO NRs (a), Fe-containing ZnO NRs (c) and their SAED patterns (b) and (d), respectively.

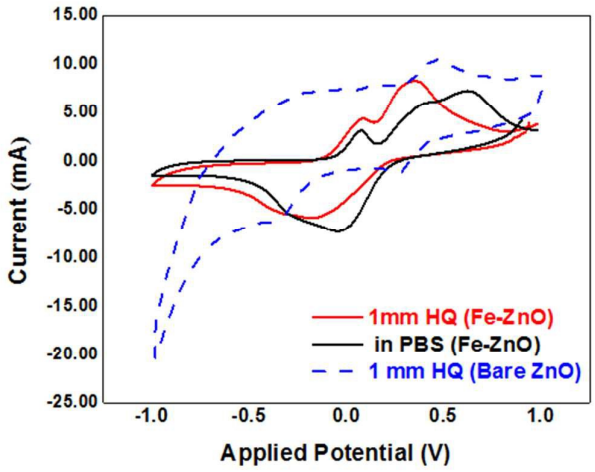

Fig. 6 Typical cyclic voltammogram sweep curve of the bare-ZnO (blue line), Fe-doped ZnO NRs modified electrode without (black line) and with 1mM of HQ (red line) in 0.1M PBS at scan rate of 50 mV/sec in the potential range of -1.0 to 1.0 V.

Sensing properties of HQ sensor based on Fe-doped ZnO NRs coated SPE

The HQ sensing properties of Fe-doped ZnO NRs were determined using cyclic voltammogram (CV) electrochemical characterization technique at a fixed scan rate of 50 mV/S in the voltage range of -1.0 to 1.0V. A typical CV curves measured in the PBS in absence and presence of 1mM of HQ are shown in Fig. 6. In the absence of HQ, CV curves show the envelope with peaks at 0.65V and -0.02V. When the sample was tested with 1mM of HQ in buffer, a redox peaks are noticed at different potential indicating that the material is able to sense the presence of HQ in buffer solution. Therefore, the CV curves

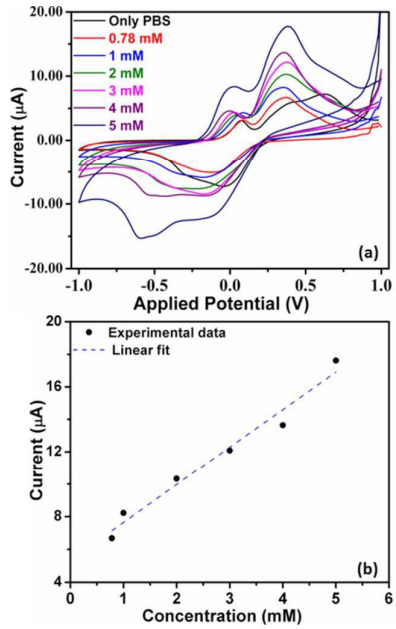

Fig. 7 Electrochemical response of the Fe-doped ZnO NRs modified electrode at different concentration of HQ ranging from 0.78 mM to 5 mM in 0. 1 M PBS (pH=7.4) at scan rate of 50 mV/sec in the potential range of -1.0 to 1.0 V (*vs.* Au electrode) and (b) calibration curve for HQ sensing.

Dalton Transactions Accepted Manuscript

This journal is © The Royal Society of Chemistry 20xx

Please do not adjust margins

Table 1. Comparison summary of the performances of HQ electrochemical sensors fabricated based on the utilization of various materials as electron mediators.

Electrode Materials	Sensitivity	Detection Limit (M)	LDR (M)	Ref.
Graphene modified GCE	-	1.5×10^{-8}	1.0×10^{-6} to 5.0×10^{-5}	15
Platinum and graphene modified GCE	1.38 μA μM^{-1} cm^{-2}	1.2×10^{-5}	20×10^{-6} to 150×10^{-6}	30
Cobalt hydroxide modified GCE	-	5×10^{-7}	5.0×10^{-6} to 125×10^{-6}	31
Copper hexacyanoferrate on Silicon electrode	-	2.2×10^{-6}	10×10^{-6} to 100×10^{-6}	32
Poly(p-aminobenzoic acid) modified GCE	-	4×10^{-5}	1.2×10^{-6} to 600×10^{-6}	33
Graphene-chitosan modified GCE	-	75×10^{-4}	1×10^{-6} to 300×10^{-6}	34
MWCNT modified GCE	-	75×10^{-4}	1×10^{-6} to 100×10^{-6}	35
Poly(thionine) modified GCE	1.8 μA μM^{-1} cm^{-2}	30×10^{-3}	1×10^{-6} to 120×10^{-6}	36
Reduced graphene oxide and MWCNT modified GCE	-	2.6×10^{-6}	8×10^{-6} to 391×10^{-6}	37
Ultrathin CdSe modified GCE	-	11×10^{-3}	0.6×10^{-6} to 1500×10^{-6}	38
L-Cys/Au SAMs	-	4.0×10^{-7}	2.0×10^{-6} to 2.0×10^{-4}	39
Dinuclear copper (II) complex in carbon paste	-	3.0×10^{-7}	6.0×10^{-5} to 2.5×10^{-3}	40
β-Cyclodextrin/Poly(N-Acetylaniline)/CNT Composite modified GCE	-	8×10^{-7}	1×10^{-6} to 5×10^{-3}	41
Fe-doped ZnO NRs	18.60 μA mM^{-1} cm^{-2}	0.51×10^{-6}	0.78 mM - 5 mM	This work

were obtained at increasing concentrations of HQ (0.78 to 5 mM). Fig. 7 shows the typical CV curves with increasing anodic and cathodic peak current at increasing concentrations of HQ. In the CV of only PBS, an oxidation peak is seen at 0.62V and reduction peak is at -0.02V, which is due to the material itself with possible functional bonds and surface defects (as seen from the FTIR and FESEM observations). When CV curve was obtained with HQ, the effect is seen as shift in redox peak potentials at 0.36V and -0.1V. The redox peaks are found separated with separation potential (ΔEp) of 0.46V, which is less than unity indicating the quasi reversible process of HQ interaction with Fe-ZnO. A systematic change in the redox peak currents are noticed with increasing HQ concentration.

Fig. 7b shows the increase in the anodic peak current with different HQ concentrations, where peak currents increased linearly with increasing HQ concentration. The estimated sensitivity from this curve is 18.60 μA/mM-cm^2 with linearity over 96%. From Fig. 7, it is realized that the oxidation and reduction of HQ to benzohydroquinone takes place at the electrode surface, as shown in Fig. 1 and as reported elsewhere.[26] This clearly confirms that the Fe-doped ZnO NRs coated on SPE acts as an efficient electron mediator.

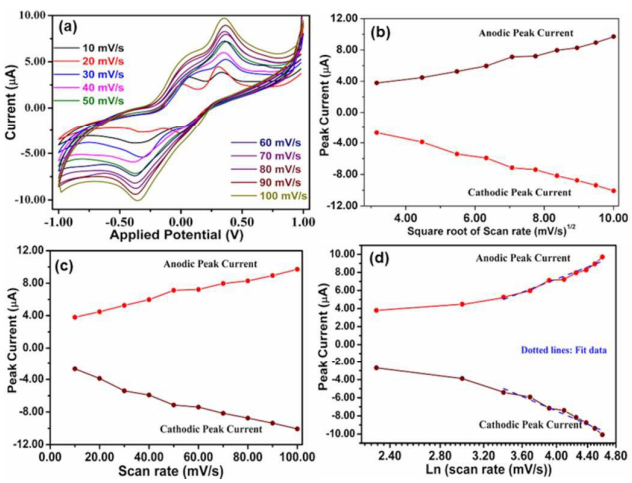

Fig. 8 (a) Cyclic voltammograms obtained at various scan rates of 10-100 mV/s for Fe-doped ZnO NRs modified electrode in 0.1 M PBS (pH=7.4), containing 3 mM HQ. (b) Plot for the anodic and cathodic peak current versus the square root of the scan rates (v1/2) in same solution; (c) Plot for the anodic and cathodic peak current versus the scan rates (v) in same solution and (d) Plot for the anodic and cathodic peak current versus the natural Log of scan rates (Lnv) in same solution.

To determine the limit of detection (LOD), the standard deviation value obtained from the calibration curve shown in Fig. 7b was multiplied, 3 times i.e 3.93 μA*3=11.79 μA and then to this value to the peak current without HQ (i.e. offset value = 5.5 μA) i.e. 5.5μA + 11.79 μA = 17.29 μA. This value was projected back to X-axis by the interpolation of the line that connects the offset with the first measured point (0.78mM) corresponding to 6.6 μA. The intercept on X-axis was then taken as LOD value, which is 0.51 μM. List of reported sensor parameters using different material is listed in Table 1 for comparison of the performance of the fabricated HQ chemical sensor. It is clear that the fabricated sensor has superior performance than reported sensors in the literature.[15,27-38]

For understanding the charge transfer characteristics of the Fe-doped ZnO NRs, scan rate study was carried out and CV curves were obtained at various scan rates (10, 20, 30, 40, 50, 60, 70, 80, 90 and 100 mV/s) in 1 mM HQ solution. A systematic change in CV envelop, the oxidation/reduction peak currents is noticed with increasing scan rate which are shown as Fig. 8a, which shows a linear variation with the scan rate indicating the redox reaction at the working electrode, which is a surface-controlled process since the adsorption-controlled current contributes majorly to the peak current. To understand the diffusion controlled process, the anodic/cathodic peak currents were plotted as square root of the scan rate ($v^{1/2}$), which exhibited a linear response indicating a diffusion-controlled process due to fast electron transfer mechanism, as can be seen in Fig. 8(b) and (c). Further, the variation in the anodic/cathodic peak currents

Dalton Transactions Accepted Manuscript

with natural Log of scan rates (Ln*v*), Fig. 8d, shows a linear relationship of peak currents with scan rate (Ln*v*) with a linearity of 95%, indicating the diffusion-controlled reaction occurring on the electrode. Also the slope of the curve is close to the theoretical value, further confirming that the electrode reaction was a diffusion-controlled process.[13]

Conclusions

In conclusion, we synthesized well-crystalline Fe-doped ZnO NRs by hydrothermal process at low temperature and characterized in detail, which confirmed the high-density growth, and wurtzite hexagonal phase with good optical and functional properties. The Fe-ZnO NRs were used to modify the SPE as efficient electron mediators for HQ electrochemical sensing and tested upto the safe limit of HQ i.e. 5mM. The fabricated sensor exhibited sensitivity of 18.60 μA mM^{-1} cm^{-2} and very low experimental detection limit of 0.51 μM. From this study it can be concluded that such materials can be used for developing various types of electrochemical sensors.

Acknowledgements

This work was supported by the Ministry of Higher Education, Kingdom of Saudi Arabia for the research grant (PCSED-021-13) under the Promising Centre for Sensors and Electronic Devices (PCSED) at Najran University.

References

1 F. Arduini, C. Zanardi, S. Cinti, F. Terzi, D. Moscone, G. Palleschi and R. Seeber, *Sens. Actuators B: Chem.,* 2015, **212**, 536.
2 B. Molinero-Abad, M. Asunción Alonso-Lomillo, O. Domínguez-Renedo and M. Julia Arcos-Martínez, *Sens. Actuators B: Chem.,* 2015, **211**, 250.
3 Y. Xie, R. Xing, Q. Li, L. Xu and H. Song, *Sens. Actuators B: Chem.,* 2015, **211**, 255.
4 R. L. Blakley, D. D. Henry and C. J. Smith, *Food Chem. Toxicol.,* 2009, **39**, 401.
5 D. Neagu, G. Tsekouras, D. N. Miller, H. Ménard and J. T. S. Irvine, *Nat. Chem.,* 2013, **5**, 916.
6 Borges, C. Fonseca, N.P. Barradas, E. Alves, T. Girardeau, F. Paumier, F. Vaz and L. Marques, *Electrochim Acta,* 2013, **106**, 23.
7 (a) Ed. Ahmad Umar, Y.B. Hahn, "Metal oxide nanostructures and their applications" American Scientific Publishers, Los Angeles, USA (2010); (b) T. Athar, Metal oxide nanopowder, Emerging Nanotechnologies for Manufacturing (Second Edition) ed. W. Ahmed and J. Mark Jackson, (William Andrew (Elsevier), MA, USA, 2015). Chap. 14, 343.
8 S. Das and V. Jayaraman, *Prog. Mater. Sci.,* 2014, **66**, 112.
9 M. José-Yacamán and R. Mehl, *Metall. Mater. Trans. A,* 1998, **29**, 713.
10 G. George and S. Anandhan, *Mat. Sci. Semicon. Proc.,* 2015, **32**, 40.
11 J. L. O'Donoghue, *J. Cosmet. Dermatol.,* 2006, **5**, 196.
12 F. J. Enguita and A. L. Leitão, *Biomed. Res. Int.,* 2013, **2013**, 542168.
13 S. Hu, Y. Wang, X. Wang, L. Xu, J. Xiang and W. Sun, *Sens. Actuators B: Chem.,* 2012, **168**, 27.
14 J. Zou, J. Ma, Y. Zhang, L. Huang and Q. Wan, *J. Chem. Technol. Biot.,* 2014, **89**, 259.
15 H. Du, J. Ye, J. Zhang, X. Huang and C. Yu, *J. Electroanal. Chem.,* 2011, **650**, 209.
16 P. S. da Silva, B. C. Gasparini, H. A. Magosso and A. Spinelli, *J. Braz. Chem. Soc.,* 2013, **24**, 695.
17 H. S. Han, J.-M. You, H. Seol, H. Jeong and S. Jeon, *Sens. Actuators B: Chem.,* 2014, **194**, 460.
18 (a) S. Al-Heniti, Ahmad Umar, H. M. Zaki, J. Nanosci. Nanotech., 2015, **15**, 9954; (b) S. H. Kim, Ahmad Umar, R. I. Badran, H. Algarni, J. Nanoelectron. Optoelectron. 2015, **10**, 688; (c) Ahmad Umar, R. Kumar, G. Kumar, H. Algarni, S. H. Kim, J. Alloys Compounds 2015, **648**, 46
19 (a) Ahmad Umar, M.S. Akhtar, A. Al-Hajry, M.S. Al-Assiri, G.N. Dar, M. S. Islam, Chem. Engg. Journal, 2015, **262**, 588; (b) S. Kumar, G. Bhanjana, N. Dilbaghi, Ahmad Umar, Ceramic International, 2015, **41**, 3101; (c) R. Kumar; G. Kumar; Ahmad Umar, M.S. Akhtar, J. Alloys Compounds, 2015, **629**, 167
20 (a) K. Singh, A. Kaur, Ahmad Umar, G.R. Chaudhary, S. Singh, S. K. Mehta, J. Appl. Electrochem. 2015, **3**, 253; (b) Ahmad Umar, J. Nanosci. Nanotechnol. 2015, **15**, 6801; (c) Sushil Kumar Kansal, Randeep Lamba, S.K.Mehta, Ahmad Umar, "Photocatalytic Degradation of Alizarin Red S Using Simply Synthesized ZnO Nanoparticles", Mater. Lett., 2013, **106**, 385.
21 (a) M. Ahmad, J. Zhao, J. Iqbal, W. Miao, L. Xie, R. Mo and J. Zhu, *J. Phys. D: Appl. Phys.,* 2009, **42**, 165406; (b) M. Ahmad, C. Pan and J. Zhu, *J. Mater. Chem.,* 2010, **20,** 7169; (c) A. K. Behera, N. Mohapatra and S. Chatterjee, *J. Nanosci. Nanotechnol.,* 2014, **14,** 3667.
22 G.N. Dar, A Umar, S.A. Zaidi, Ahmed A. Ibrahim, M. Abaker, S. Baskoutas and M.S. Al-Assiri, *Sens. Actuators B: Chem.,* 2012, **173**, 72.
23 Y. Zhang, G.-M. Zeng, L. Tang, D.-L. Huang, X.-Y. Jiang and Y.-N. Chen, *Biosens. Bioelectron.,* 20017, **22**, 2121.
24 D. Li, J. Yang, J. Zhou, Q. Wei and F. Huang, *RSC Adv.,* 2014, **4**, 61831.
25 (a) M. Meshki, M. Behpour, S. Masoum, *J. Electroanalyt. Chem.,* 2015, **740**, 1; (b) A. Khayatian, M. A. Kashi, R. Azimirad and S. Safa, *J. Phys. D: Appl. Phys.,* 2014, **47**, 075003; (c) Q. Humayun, U. Hashim, *Adv. Mater. Research*, 2015, **1109**, 200; (d) C. O. Chey, A. Masood, A. Riazanova, X. Liu, K. V. Rao, O. Nur and M. Willander, *J. Nanomater.,* 2014, **524530**, 1; (e) M. V. Limaye, S. B. Singh, R. Das, P. Poddar and S. K. Kulkarni, *J. Solid State Chem.,* 2011, **184**, 391. (f) M.N. Rumyantseva, V.V. Kovalenko, A.M. Gaskov, T. Pagnier, D. Machon, J. Arbiol, J.R. Morante, *Sens Actuat* B, 2005, **109** 64.
26 (a) R. Wahab, S. G. Ansari, Y. S. Kim, M. Song and H. Shin, *App. Surf. Sci.,* 2009, **255**, 4891; (b) K. Sambath, M. Saroja, M. Venkatachalam, K. Rajendran and N. Muthukumarasamy, *J. Mater. Sci: Mater. Electron.*, 2012, **23**, 431.
27 (a) Y. Yang, H. Lai, C. Tao and H. Yang, *J. Mater. Sci: Mater. Electron.,* 2010, **21**, 173; (b) Y. I. Jung, B. Y. Noh, Y. S. Lee, S. H. Baek, J. H. Kim and I. K. Park, *Nanoscale Research Lett.,* 2012, **7**, 43.
28 R. A. Nyquist and R. O. Kagel, 'Infrared spectra of Inorganic Compounds'; Academic Press, Inc.: New York, London, 1971.
29 A. Umar, R. Ahmad, A. Al-Hajry, S. H. Kim, M. E. Abaker and Y.- B. Hahn, *N. J. Chem.,* 2014, **38**, 5873.
30 J. Li, C.Y. Liu and C. Cheng, *Electrochimca Acta,* 2011, **56**, 2712.
31 L. F. Fan, X. Q. Wu, M. D. Guo and Y. T. Gao, *Electrochimca Acta,* 2007, **52**, 3654.
32 H. Wu, J. Hu, H. Li and H. Li, *Sens. Actuators B: Chem.,* 2013, **182**, 802.
33 P. Yang, Q.Y. Zhu, Y.H. Chen and F.W. Wang, *J. Appl. Poly. Sci.,* 2009, **113**, 2881.

Dalton Transactions Accepted Manuscript

This journal is © The Royal Society of Chemistry 20xx

34 H. S. Yin, Q. M. Zhang, Y. L. Zhou, Q. Ma, T. Liu, L. S. Zhu and S. Y. Ai, *Electrochimca Acta,* 2011, **56**, 2748.
35 H. L. Qi and C. X. Zhang, *J. Electroanal. Chem.,* 2005, **17**, 832.
36 A. J. S. Ahammad, M. M. Rahman, G. R. Xu, S. Kim and J. J. Lee, *Electrochimca Acta,* 2011, **56**, 5266.
37 F. X. Hu, S. H. Chen, C. Y. Wang, R. Yuan, D. H. Yuan and C. Wang, *Anal. Chim. Acta,* 2012, **724**, 40.
38 X. Cao, X. Cai, Q. Feng, S. Jia and N. Wang, *Anal. Chim. Acta,* 2012, **752**, 101.
39 S. Wang and D. Du, *Sensors*, 2002, **2**, 41.
40 I. R. W. Z. de Oliveira, R. E. M. D. Osorio, A. Neves and I. C. Vieira, *Sens. Actuators B: Chem.,* 2007, **122**, 89.
41 B. Kong, T. Yin, X. Liu and W. Wei, *Anal. Lett.,* 2007, **40**, 2141.

Dalton Transactions Accepted Manuscript